Journal of Computers Vol. 31 No. 4, 2020, pp. 141-156
doi:10.3966/199115992020083104011

An Improved Multi-objective Shark Smell Optimization Algorithm for Automatic Train Operation Based on Angle Cosine and Fusion Distance

Long-Da Wang, Xing-Cheng Wang*, Kai-Wei Liu

Department of Marine Electrical Engineer, Dalian Maritime University, Dalian 116023, Liaoning, China
dmuwxc@dlmu.edu.cn

Received 21 January 2019; Revised 8 June 2019; Accepted 15 July 2019

Abstract. Aiming at the problem of easy to fall into local convergence for automatic train operation (ATO) velocity ideal trajectory profile optimization algorithms, an improved multi-objective shark smell optimization algorithm based on angle cosine and fusion distance is proposed. Firstly, an automatic train operation (ATO) multi-objective optimization model is established, which take into account the energy-saving, comfort, precise parking and punctuality of train operation process. Secondly, in order to improve the algorithm search ability, shark smell optimization algorithm (SSO) is adopted due to its powerful search mechanism. Thirdly, in order to avoid the problem that subjective parameters are selected blindly in traditional multi-objective evaluating index, the angle cosine of solution vector and target demand vector is used as evaluating index due to its objective and reasonable. Fourthly, in order to restrain the phenomenon of individual aggregation at the end of the iteration, the fusion distance takes into account the correlation and independence of multi-feature variables is used as the distance measurement, which can effectively suppress the local convergence. Finally, the MATLAB simulation results and ATO HILS (hardware-in-the-loop simulation) results show that show that the proposed improved SSO has a better optimization effect than that of the traditional optimization algorithms and their improved algorithms.

Keywords: automatic train operation, angle cosine, fusion distance, multi-objective optimization, shark smell optimization algorithm

1 Introduction

Compared to other means of transport, rail transit system has the advantage of speedy, convenience and large carrying capacity. The train operation process is an optimization problem that needs to meet many performance indicators such as energy consumption, parking punctuality, comfort and so on, and there are more than one and even infinite Pareto non-dominated solutions in the optimal solution set.

With the rapid development of rail transit, the people's demand for the comprehensive performance index of train operation process is increasingly high. The optimization result based on single optimization target can no longer satisfies the actual demand, but the research on multi-objective optimization algorithm of train operation process is relatively underdeveloped [1]. The multi-objective optimization of train operation process has multiple optimization indicators and nonlinear characteristics, and it is has various influence factors, which leads to the extreme complexity of the optimization problem. Therefore, the ATO control system using traditional optimization algorithm is difficult to obtain the optimal control sequence in numerous different control sequences. The ATO control system which can give precise control sequence for any given train parameter, line condition, constraint and optimization objective has always been the goal of the relevant scientific researchers for many years. Various control schemes have been proposed in recent works on the ATO control strategy [2-6]. To take into account both energy consumption and travel time, based on speed limit and line characteristics, a hybrid evolutionary

* Corresponding Author

algorithm based on differential evolution algorithm and simulated annealing algorithm is designed [2]. To solve multi-objective Pareto solution of the train running public transport system, a new non-linear differentiate evolution method for fuzzy membership functions of self-adaptive adjustment is proposed [3]. The tracking operation of energy saving train based on multiple optimization model is studied, which of novelty is to establish a new multi-objective model which can switch the optimization framework, to ensure the punctuality of the train tracking operation while reducing energy consumption [4]. In order to save energy consumption as much as possible, the best ATO speed curve of the subway train considering regenerative brake is designed [5]. An energy efficiency calculation method for Chinese mainline railways is proposed and verified [7]. However, there is a little related literature published about the genetic shark smell optimization algorithm based on angle cosine and fusion distance measurement about ATO control system.

To resolve the aforementioned problem, the multi-objective genetic shark smell optimization algorithm of automatic train operation based on angle cosine and fusion distance. The main advantages of the proposed algorithms are summarized as follows:

(I) Shark Smell Optimization, SSO is a new swarm intelligence optimization algorithm proposed by Abedinia O in 2016. Compared to conventional optimization algorithms such as particle swarm, based on the shark's spiral hunting mechanism, the shark smell algorithm is characterized by few parameters, so it has a strong local search capability.

(II) For the conventional multi-objective unification target method such as linear weighting, there is a problem that subjective parameters are selected blindly in the calculation. Because the target demand vector can be selected objectively according to the actual situation, the angle cosine of solution vector and target demand vector as evaluating index is more objective and reasonable.

(III) Train running process optimization is an extremely complicate optimization decision problem, in the late iteration, it is easy to fall into local convergence. Therefore, in the later period of the optimization iteration, it is necessary to filter the individuals who are close to the extremum but not are sufficiently optimized to prevent these individuals from confining the population to a local area. However, using Euclidean distance or Mahalanobis distance as the distance measure cannot accurately reflect the actual distance. In this paper, a method of local convergence inhibition is proposed by using the fusion distance based on Mahalanobis distance and Euclidean distance as the distance measure indicator in the later stage of the iterative optimization process to enhance the global convergence performance of the optimization algorithm.

This paper is organized as follows: Section 2 introduces the multi-objective model of train operation process. Section 3 presents the concept of multi-objective optimization of train operation. Section 4 illustrates the improvement strategy of the improved multi-objective shark smell optimization algorithm based on angle cosine and fusion distance. Section 5 provides the simulation results to illustrate the proposed method. Section 6 concludes this article.

2 Multi-objective Model of Train Operation Process

2.1 Constraint Model

The constraint model based on general equation of the train motion is shown below:

$$\begin{cases} Mv\dfrac{dv}{ds} = u_f F_t\left(u,v\right) - R\left(v,s\right) - u_b B_r\left(u,v\right) \\ \dfrac{dt}{ds} = \dfrac{1}{v} \\ v_k \le v_{\lim\_k} \\ s_q = 0, \left|s_z - D\right| < \Delta s \end{cases} . \tag{1}$$

Where t represents the actual running time of the train, s denotes the actual position of the train, M is the effective quality of the train, $u_f F_t\left(u,v\right)$ and $u_b B_r\left(u,v\right)$ are the traction force and braking force of the current velocity, $R\left(v,s\right)$ is the additional resistance of the train determined by the current speed and position of the train. s_q and s_z are the positions of the front and back stations respectively, v_k and $v_{\lim\_k}$ are the running speed and the limit speed of the preset position, Δs is the limit parking error [8]. The control modes of maximum traction, partial traction, idle running, partial braking and maximum braking are adopted in the paper, which are represented by $[1,0.5,0,-0.5,-1]$. u represents the train control sequence that are the decision variables, u_f and u_b are the traction and braking coefficients which needs to satisfy the following constraints.

$$\begin{cases} u_f, u_b \in [0,1] \\ u_f \cdot u_b = 0 \end{cases} . \tag{2}$$

2.2 Energy Consumption Model

The train energy consumption is expressed as the energy consumed by overcoming resistance during the whole process and the specific calculation formula is

$$K_E = \sum_{i=1}^{n} \left(Ma_i - R_i \right)\left(s_i - s_{i-1} \right) . \tag{3}$$

Where K_E is the measure of the energy consumption, a_i is the acceleration of the i th condition, s_i is the position of the i th condition, R_i is the resistance of the i th condition.

2.3 Comfort Model

The comfort level can reflect the quality of passengers' riding, which is expressed by the sum of the absolute value of the difference of the acceleration of the adjacent working conditions in the running process, and the specific calculation formula is

$$K_A = \sum_{i=2}^{n} \left| a_i - a_{i-1} \right| . \tag{4}$$

Where K_A is the measure of comfort, a_i is the acceleration of the i th condition.

2.4 Punctuality Model

The train punctuality is the absolute value of the difference between the actual running time and the prescribed running time and the specific calculation formula is as follows:

$$K_T = \left| \sum_{i=1}^{n} \left[\left(\sqrt{2a_i \left(s_i - s_{i-1} \right) + v_{i-1}^2} - v_{i-1} \right) \Big/ a_i \right] - T \right| . \tag{5}$$

Where K_T is the measure of punctuality.

2.5 Multi-objective Optimization Model

The multi-objective optimization model of the train operation is established based on energy consumption, comfort and running time as the optimization goals.

$$\begin{cases} F(u) = (K_E(u), K_A(u), K_T(u)) \\ \min \{ F(u) \} \end{cases} . \tag{6}$$

Where min denotes the minimum value of $F(u)$, which is the minimum value of each sub-objective function of $F(u)$.

3 Concept of the Multi-objective Optimization of Train Operation

3.1 Optimal Solution of the Multi-objective Optimization of Train Operation

The target vector of the multi-objective optimization problem is $F(x)=(f_1(x),f_2(x),\cdots,f_k(x))$, and the optimization model can be expressed as

$$\begin{cases} & \min\{F(x)\} \\ s.\,t. & g(x)\le 0, i=1,2,\cdots,m \\ & x=(x_1,x_2,\cdots,x_n), x\in D^* \end{cases} . \tag{7}$$

Where k is the number of optimization targets, x is the decision variable, $g(x)$ is the inequality constraint for x. x'' is the absolute optimal solution, and if and only if any $x'\in D^*$, $F(x'')$ is superior to $F(x')$ [9].

The multi-objective optimization of train operation is to find the optimal train operation sequence $\{o_1,o_2,\cdots,o_k\}$ by using some optimization methods for any given train parameters, line conditions and constraints, where $o_i=(u_i,p_i)$ represents the i th operation mode, u_i is the train control mode, p_i is the switching position ($i\in[1,2,...,k]$). The train control sequence $\{o_1,o_2,\cdots,o_k\}$ is adopted to control the train operation, which optimizes the indexes such as energy consumption, punctuality and comfort to the maximum extent.

3.2 Shark Smell Optimization Algorithm

As the best hunter in nature, sharks have the foraging behavior that goes forward and rotates, which can be extremely efficient in finding prey. The optimization algorithm for simulating shark foraging is a highly efficient optimization algorithm. For any given location, the sharks move at a speed to the particle that have the more intense scent, so the NP initial velocity vectors are defined.

$$\left[V_1^1,V_2^1,..........,V_{NP}^1\right] . \tag{8}$$

The shark has inertia when it swims, so the velocity formula of each dimension is defined as follows:

$$V_{i,j}^k=\eta_k\cdot R1\cdot\left.\frac{\partial(OF)}{\partial x_j}\right|_{x_{i,j}^k}+\alpha_k\cdot R2\cdot v_{i,j}^{k-1} . \tag{9}$$

Where $j=(1,2,\cdots,ND)$, $i=(1,2,\cdots,NP)$, OF is the objective function; k represents the number of phases. The shark may not reach the speed indicated by the gradient function at each stage, so set $\eta_k\in[0,1]$. $R1$ and R_2 are the random number between $[0,1]$, which is called the gradient item. α_k is also the random number between $[0,1]$, which is called the inertia coefficient or the rate of momentum change.

The speed of the shark is bounded, and its speed limit formula is described as

$$\left|v_{i,j}^k\right|=\min\left[\left|\eta_k\cdot R1\cdot\left.\frac{\partial(OF)}{\partial x_j}\right|_{x_{i,j}^k}+\alpha_k\cdot R2\cdot v_{i,j}^{k-1}\right|,\left|\beta_k\cdot v_{i,j}^{k-1}\right|\right] . \tag{10}$$

Where $j=(1,2,\cdots,ND)$, $i=(1,2,\cdots,NP)$, $k=(1,2,\cdots,k_{\max})$, β_k is the speed limit factor of the k phase, the magnitude of $v_{i,j}^k$ can be obtained from the formula above. The shark has a new position Y_i^{k+1} due to moving forward, and Y_i^{k+1} is determined by the previous speed and position, which is expressed as

$$Y_i^{k+1} = X_i^k + V_i^k \cdot \Delta t_k \ . \tag{11}$$

Where $i = (1, 2, \cdots, NP)$, $k = (1, 2, \cdots, k_{\max})$, Δt_k represents the time interval in the k phase. Each velocity component of the velocity v_i^k is obtained from the above formula (11). In addition to moving forward, sharks usually rotate along their path to look for stronger odor particles and improve their direction of movement, which is a real way of moving. The rotating shark moves in a closed interval which is not necessarily a circle. From the point of view of optimization, sharks implement local search at each stage to find better candidate solutions. The search formula for this position is as follows:

$$Z_i^{k+1,m} = Y_i^{k+1} + R3 \cdot Y_i^{k+1} \ . \tag{12}$$

Where $m = (1, 2, \cdots, M)$, $R3$ is the random number between $[-1,1]$, M represents the number of points at each stage of the location search. If the shark finds a stronger scent point in the rotation, it moves toward the point and continues the search path. The location search formula is described as follows:

$$X_i^{k+1} = \arg\max \left\{ OF(Y_i^{k+1}), OF(Z_i^{k+1,1}), \cdots, OF(Z_i^{k+1,M}) \right\} . \tag{13}$$

As can be seen from the above formula, Y_i^{k+1} is obtained from the linear movement and $Z_i^{k+1,m}$ is obtained from the rotation movement. Sharks will choose the candidate solution X_i^{k+1} with higher evaluation index value as shark's next location

3.3 Linear Weighted Target Method

Compared with the multi-objective optimization problem, the single objective optimization problem is easier to solve. It is a practical and effective way to transform the original multi-objective optimization problem into a single objective optimization problem. In order to eliminate the negative influence caused by the difference between dimensions and orders of magnitude, the data needs to be normalized. The calculation formula of the normalized linear weighted target $F'(x)$ can be expressed as

$$\begin{cases} F'(x) = \sum_{i=1}^{k} \omega_i' \omega_i'' f_i(x) \\ \omega_i'' = \dfrac{f_i(x) - \min\left(f_i(x)\right)}{\max\left(f_i(x)\right) - \min\left(f_i(x)\right)} \end{cases} . \tag{14}$$

Where ω_i' represents the intrinsic weight factor ($\sum_{i=1}^{k} \omega_i' = 1$), which reflects the relative importance of the i th optimization goal. ω'' denotes the correction weight factor, which eliminates the negative influence caused by the difference of dimensions and orders of magnitude for the i th optimization goal. $\max$ and $\min$ respectively represent the maximum and minimum values of the function. However, the selection of the intrinsic factor of the linear weighted target method lacks the specific theoretical basis, so there is certain subjective limitation in this method.

3.4 The Method to Suppress Local Convergence

Considering that the optimization algorithm is easy to fall in the local convergence in the later period, there is a large number of individuals in the smaller neighborhood of the extreme individual, and some of the individuals need to be replaced before the next iteration, to prevent these individuals from confining the population to the local area. An improved strategy in optimization algorithm, which combines with the idea of genetic algorithm at the later evolution stage, is put forward, to improve the optimization effect of the algorithm by filtering the poor individuals in the neighborhood of the extreme individual. The flowchart of the improved optimization algorithm is shown in Fig. 1.

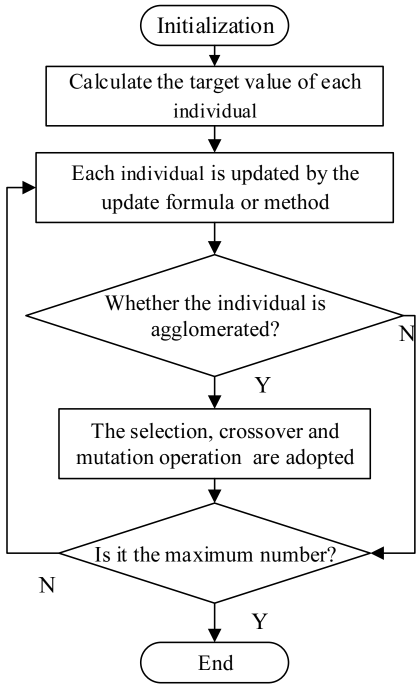

Fig. 1. The flowchart of the improved optimization algorithm which suppresses local convergence

The judging formula of the population gathering in the individual extremum can be expressed as

$$\forall Dis\left|\vec{p}_i - \Omega(\vec{p})\right| \le \varepsilon \ . \tag{15}$$

Where $\Omega(\vec{p})$ represents the sample space composed of individual extreme values of particles, $Dis\left|A-B\right|$ denotes the distance from sample A to sample space B, ε is the threshold. Euclidean distance formula is generally used to measure the distance between the two samples, and the specific calculation formula is as follows.

$$ED = \left[\sum_{n=1}^{k}\left|x_{i,n} - x_{j,n}\right|^2\right]^{1/2} \ . \tag{16}$$

Where ED is the Euclidean distance, x_i and x_j represent two samples to be examined, $n \in [1,2,...,k]$ denotes the dimension of the sample.

For the train multi-objective control optimization problem, the calculation formula of Euclidean distance of differences between two different control sequences is described as follows.

$$ED(u_1,u_2) = \left[\omega_v \times \sum_{i=1}^{D}\left|v_i(u_1) - v_i(u_2)\right|^2 + \omega_t \times \sum_{i=1}^{D}\left|t_i(u_1) - t_i(u_2)\right|^2\right]^{1/2} \ . \tag{17}$$

Where $ED(u_1,u_2)$ denotes the Euclidean distance of differences caused by using u_1 and u_2 to control train operation, $v_i(u)$ and $t_i(u)$ represent the instantaneous velocity and current time of the i th operating point by using u to control train operation. ω_v and ω_t express the correction weight factor for speed and distance, which eliminates the negative influence caused by the difference of dimensions and orders of magnitude for the time and speed.

4 Method of Improved Shark Smell Optimization Algorithm

4.1 Angle Cosine

For multi-objective optimization problems, there is an angle between the target vector of any solution and the target demand vector in the solution space, and the angle cosine is less than or equal to 1. The target demand vector is the target vector of the desired optimal solution which may not be the final optimization solution. But the target demand vector plays an active role in guiding the global convergence of the optimization algorithm in the process of iterative optimization. The calculation formula of the angle cosine between the solution target vector *T* and the target demand vector *C* is expressed as

$$\gamma = \frac{(T,C)}{\|T\| \bullet \|C\|} = \frac{\sum_{i=1}^{k} t_i \bullet c_i}{\sqrt{\sum_{i=1}^{k} t_i^2} \bullet \sqrt{\sum_{i=1}^{k} c_i^2}} . \quad \textbf{(18)}$$

Where γ is the angle cosine, (T,C) represents the dot product between the target vector *T* and the target demand vector *C*, $\|A\|$ is the length of vector *A*, $\bullet$ denotes the numerical multiplication, t_i and c_i express the normalized value of the *i* th optimization goal of the solution target vector *T* and the target demand vector *C*.

The normalization is to eliminate the negative influence caused by the difference between dimensions and orders of magnitude. The specific angle cosine of the target vector and the target demand vector is shown in Fig. 2.

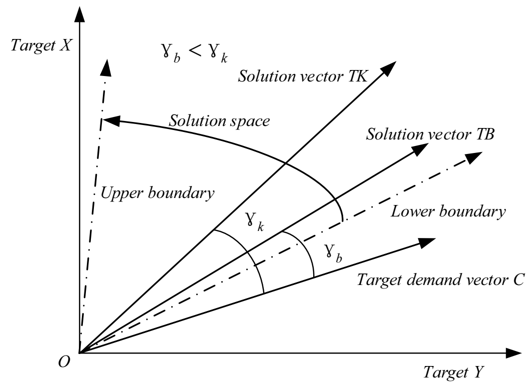

Fig. 2. The angle cosine diagram of the target vector and the target demand vector

Where the two axes represent two optimization objectives, the three solid lines in the axes respectively denotes the solution target vector *TK*, the solution target vector *TB* and the target demand vector *C*. The arc expresses the solution space, the two dotted lines in the axis represent the boundary of the solution space. The intersection angles represented by the angles *k* and *b*, the intersection angle cosines are expressed by γ_k and γ_b .

4.2 Fusion Distance

Mahalanobis distance can accurately calculate the covariance distance between two samples. The formula of Mahalanobis distance between the sample $\boldsymbol{X}$ to be examined and the basic space set $\boldsymbol{Y}$ is expressed as

$$
\begin{aligned}
&d\left(\boldsymbol{X},\boldsymbol{Y}\right)=\sqrt{(\boldsymbol{X}-\overline{\boldsymbol{Y}})'\boldsymbol{\Sigma}^{-1}(\boldsymbol{X}-\overline{\boldsymbol{Y}})}=\sqrt{(\boldsymbol{X}-\overline{\boldsymbol{Y}})'\boldsymbol{\Sigma}_{Y}^{-1}(\boldsymbol{X}-\overline{\boldsymbol{Y}})}\ .\\
&\boldsymbol{\Sigma}=Cov(\boldsymbol{X},\boldsymbol{Y})=E\left[\left(\boldsymbol{X}-E\left(\boldsymbol{X}\right)\right)\left(\boldsymbol{Y}-E\left(\boldsymbol{Y}\right)\right)\right]\ .\\
&=\begin{bmatrix} Cov\left(x_1,y_1\right) & Cov\left(x_1,y_2\right)\cdots Cov\left(x_1,y_j\right)\\ Cov\left(x_2,y_1\right) & Cov\left(x_2,y_2\right)\cdots Cov\left(x_2,y_j\right)\\ \vdots & \vdots \quad \ddots \quad \vdots\\ Cov\left(x_j,y_1\right) & Cov\left(x_j,y_2\right)\cdots Cov\left(x_j,y_j\right)\end{bmatrix}.
\end{aligned}
\quad \textbf{(19)}
$$

Where is the expected matrix of the covariance matrix for the basic space set $\boldsymbol{Y}$, $\boldsymbol{\Sigma}$ is the expected matrix of the covariance matrix for the basic space set $\boldsymbol{Y}$, $\overline{\boldsymbol{Y}}$ and $\boldsymbol{\Sigma}_Y$ are the mean matric and covariance matric of $\boldsymbol{Y}$ [10-12].

When the correlation between the characteristic variables is fuzzy, the classical Mahalanobis distance and Euclidean distance cannot effectively calculate the distance between the sample $\boldsymbol{X}$ to be examined and the basic space set $\boldsymbol{Y}$, but the method proposed by literature [13] can solve this problem. The distance fusion is the combination of Mahalanobis distance and Euclidean distance, taking into account the independence and relevance of the characteristic variables, which can effectively improve the accuracy of distance calculation. The specific calculation formula of the fusion distance is expressed as

$$
\begin{cases}
d_{\text{Mix}}=\omega\times MD(\boldsymbol{X},\boldsymbol{Y})+\left(1-\omega\right)\times ED(\boldsymbol{X},\boldsymbol{Y})\\
C_Y=\begin{bmatrix}\rho_{Y_1Y_1} & \rho_{Y_1Y_2}\cdots\rho_{Y_1Y_n}\\ \rho_{Y_2Y_1} & \rho_{Y_2Y_2}\cdots\rho_{Y_2Y_n}\\ \vdots & \vdots\ \ddots\ \vdots\\ \rho_{Y_nY_1} & \rho_{Y_nY_2}\cdots\rho_{Y_nY_n}\end{bmatrix}\\
\omega=\sqrt{1-\left|C_Y\right|}
\end{cases}.
\quad \textbf{(20)}
$$

Where d_{Mix} represents the fusion distance, MD denotes the Mahalanobis distance, C_Y expresses the correlation coefficient matrix of the sample set $\boldsymbol{Y}$, n is the number of samples in the sample set $\boldsymbol{Y}$, $Y_i\left(i=1,\cdots,n\right)$ is the sample in the sample set $\boldsymbol{Y}$, ρ is the correlation coefficient. Because MD takes into account the correlation between variables, it is fused by the weight ω with the relevant information, and ED is fused by $1-\omega$ [13].

4.3 Improved Strategy

Because the search performance of the traditional optimization algorithm is not strong enough, the shark smell algorithm is used as optimization algorithm in the paper. There is a problem of blind choice of subjective parameters in the linear traditional unified goal method, so the multi-objective angle cosine is used as good and bad evaluation criterion of the solution. Because the Euclidean distance and Mahalanobis distance cannot accurately measure the actual distance between the sample $\boldsymbol{X}$ to be examined and the basic space set $\boldsymbol{Y}$, the fusion distance is used to determine whether the particle swarm gathers in the extremum particles in this paper. The flowchart of the improved shark smell optimization algorithm based on angle cosine and fusion distance is shown in Fig. 3.

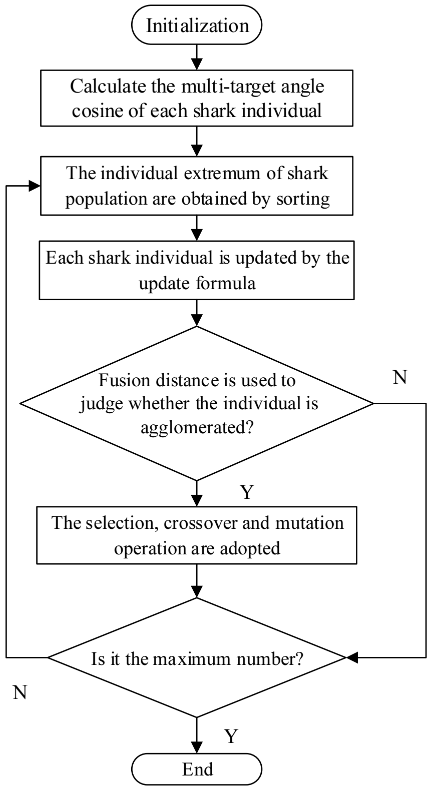

Fig. 3. The flow chart of shark smell optimization algorithm based on angle cosine and fusion distance

5 Simulation Experiment

5.1 Initialization Parameters

Considering the convergence speed and optimization effect of the algorithm, the following initialization parameters are given based on the relevant scientific literature, field experience and simulation results of multiple experiments. Simulation optimization results must satisfy the following conditions: the train instantaneous speed cannot surpass the speed limit, the train must finish the whole course, the parking error is less than 0.2m. The parameters of shark smell optimization algorithm are set as follows: the maximum number of iterations is 200, the random number $R1=0.4$, $R2=0.3$, $R3=0.25$, $\eta_k=0.2$, the inertia coefficient α_k is 0.15. The multi-objective optimization parameters of the simulation example of Dalian subway line 12 are set as follows: when the scheduled running time is 185s, $K_E \in [80000,130000]$, $K_A \in [13,30]$, $K_T \in [0,0.2]$, the intrinsic weight factors ω_1', ω_2' and ω_3' are respectively 0.5, 0.3, 0.2, the target demand vector is $[85000,13.5,0.05]$.

5.2 Relevant Data of Simulation Test

In this paper, No.12 metro vehicle of Dalian is selected as the research object. The running line of Dalian rail transit line 12 is from Lvshun New Port to Tieshan town, the interval of which is 2.94 kilometers, with two long down slopes and a long up slope. The basic properties of the train are shown in Table 1, the traction characteristics is shown in formula 15, and ramp parameters and train speed limit are shown in Fig. 4.

Table 1. The basic properties of the metro line 12 in Dalian.

Parameter name	Parameter characteristics
Maximum design speed (km/h)	80
Schedule time (s)	185
Train weight /(t)	211
Marshalling form	2 motor 2 trail
Mean starting acceleration (m/s^2)	(0～35km/h)≥1.0
Mean acceleration (m/s^2)	(0～80km/h)≥0.6
Mean barking deceleration (m/s^2)	(80～0km/h)≥1.0
Rotary mass coefficient (γ)	0.06

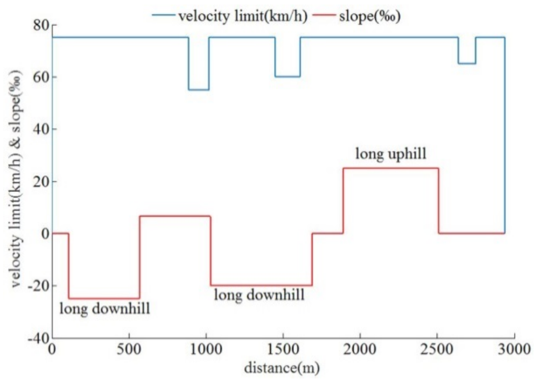

Fig. 4. The ramp parameters and speed limit of the metro line 12 in Dalian

$$\begin{cases} F(v) = F_{\max} & v_q \le v \le v_c \\ F(v) = P_{\max} / v & v_c \le v \le v_d \\ F(v) = P_{\max} \times v_d / v^2 & v_d \le v \le v_{\max} \end{cases} . \tag{21}$$

Where $F(v)$ is the traction of vehicles, $F_{\max}$ is the vehicle's maximum traction, $P_{\max}$ is the maximum traction power of the vehicle, v_d is the switching speed of the constant power zone and the reduced power zone, v_q is the switching speed of the traction starting region and constant torque region, $v_{\max}$ is the maximum design speed.

5.3 MATLAB Simulation Results and Analysis

According to Dalian No.12 subway train running environment, the optimal solutions are obtained by using the traditional improved evolutionary algorithm (multiobjective evolutionary algorithm based on decomposition, MOEA/D) [14], traditional improved shark smell optimization algorithm (chaotic shark smell optimization, CSSO) [15], the improved shark smell optimization algorithm proposed in this paper (ISSO). The MATLAB simulation results are shown in Fig. 5 to Fig. 8 and Table 2 to Table 3.

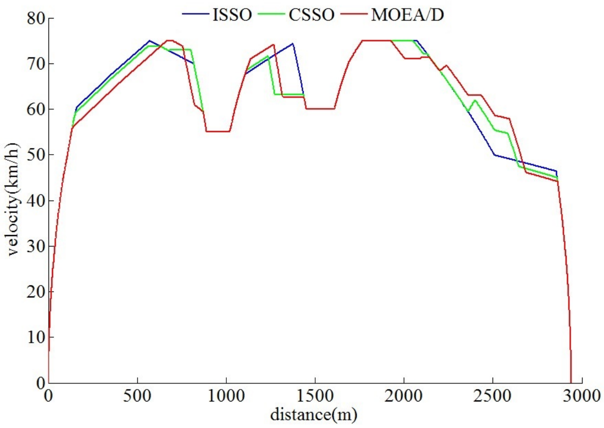

Fig. 5. The velocity distance profile of optimal results

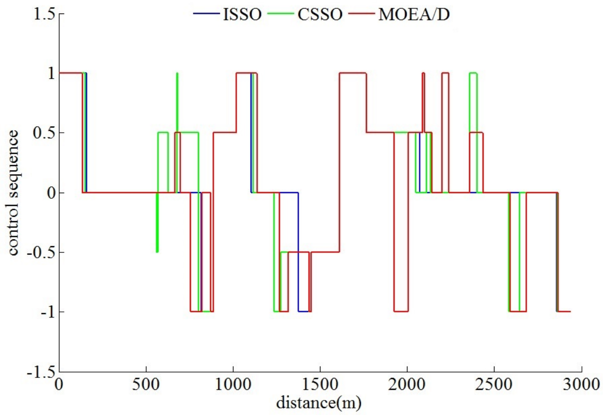

Fig. 6. The operating condition distance graph of optimal results

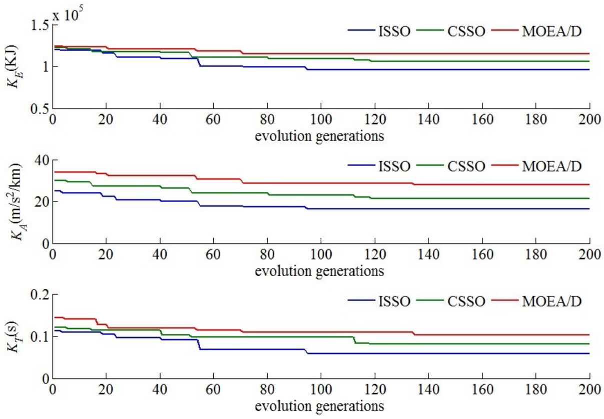

Fig. 7. Iterative convergence curves of each optimization objectives of different algorithms

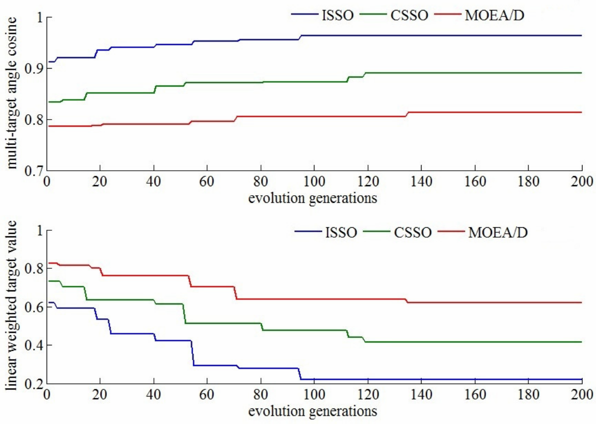

Fig. 8. Iterative convergence curves of the unified goal of different algorithms.

Table 2. Optimization results of different algorithms

Algorithm	Energy cosumption	Actual time	Comfort level	parking error
ISSO	95690KJ	185.0586s	5.5544m/s^2/km	0.0894m
CSSO	105833KJ	185.0814s	7.2703m/s^2/km	0.0915m
MOEA/D	104539KJ	185.1012s	9.5116m/s^2/km	0.1127m

Table 3. Evaluate results of different algorithms

Algorithm	Angle cosine	Linear weighted target
ISSO	0.9629	0.2215
CSSO	0.8893	0.4142
MOEA/D	0.8124	0.6208

As can be seen from the Table 2, The optimization solution obtained by the ISSO is superior to that of CSSO and MOEA/D, and three indexes of energy saving, punctuality and comfort have improved considerably. This paper selects the running line in the hilly of Dalian lvshun district, and the hilly region is the typical characteristics of Dalian. When the train is running in such a terrain, the control sequence should be concise, and the train speeds up in the long down slope and slows down in the long up slope as much as possible, which can save energy and avoid turbulence. It can be seen from the Fig. 6 and Fig. 7, the ISSO can obtain extremely simple control sequence and make the most of long down and up slopes. According to the iterative convergence curves of Fig. 8 and Fig. 9, the convergence rate of ISSO is faster than that of CSSO and MOEA/D. Even in the middle and late iterations, the algorithm of ISSO has a strong ability of global optimization.

5.4 ATO HILS Results and Analysis

MATLAB simulation is a pure software simulation technology, which lacks real hardware objects in automatic train operation (ATO), so it cannot truly reflect data interaction, transformation and processing in the actual operating process. In order to further verify algorithm performance, this paper adopts a HILS technology based on dSPACE. HILS technology is a new kind of semi-physical simulation technology which writes the optimization algorithm and the control algorithm into the kernel chips of the controller and the optimizer respectively, and it is based on the semi-physical simulation environment of the train running process to verify the performance of the train. Because HILS contains real on-board physical hardware equipment, its simulation environment can truly reflect the following three major problems.

(1) Due to the use of sensors, the sampling accuracy is limited and the speed monitoring is not accurate enough.

(2) Communication 'network' signal delay and packet loss are caused by the transmission and interaction of "network" signal in the simulation environment.

(3) Because the transmission and interaction of 'electrical' signals in the simulation environment will lead to step disturbances in the control process, the control system will be unstable.

It can be seen that HILS can provide a simulation environment extremely close to the real scene of automatic train operation, so it is highly valued by relevant researchers. The simulation topology diagram of HILS is shown in Fig. 9.

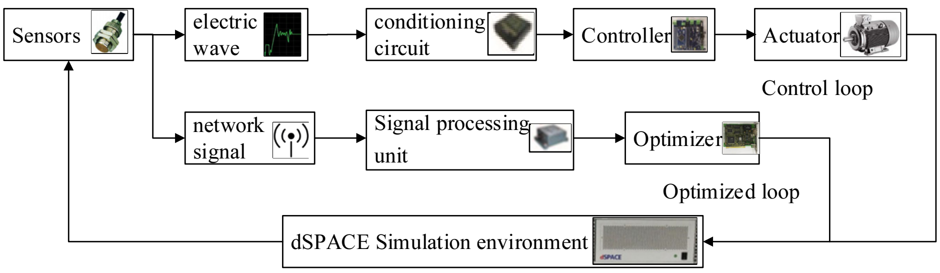

Fig. 9. The simulation topology diagram of HILS

Fig. 9 includes 'Controller loop' with 'Controller' as core and 'Optimized loop' with 'Optimizer' as core, and the core chip of the controller is 'TMS320F28335'. The processor of 'dSPACE Simulation environment' is DS1006, which is used to simulate the real scene of ATO. Sensors are used to collect a series of real data or semi-physical simulation data such as control instructions, train speed, motor current, etc. in semi-physical environment. 'Actuator' is the actuator in ATO, mainly including inverter, rectifier and traction motor, whose rated power is generally the real $A_{s,p}$ ($A_{s,p}$ is the simulation proportional coefficient of the actuator, which is 1/2000 in this paper). The physical pictures of some major ATO

HILS hardware devices adopted in this paper are shown in Fig. 10.

(a) Signal processing unit

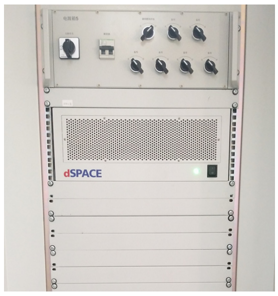

(b) dSPACE Simulator

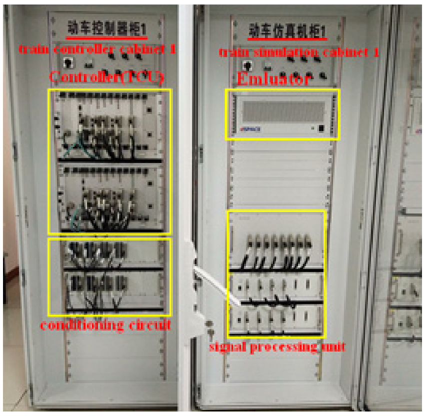

(c) Cabinets of function integration

Fig. 10. The diagram of major ATO HILS hardware

The traditional ATO MATLAB simulation environment is an extremely ideal situation and it is a special case that greatly simplifies the actual automatic train operation. Although this idealized simplification is reasonable, it will inevitably result in a considerable deviation from the actual automatic train operation. Therefore, in actual situation, the optimization effect of some improved algorithms for automatic train operation cannot achieve the effect of traditional simulation.

In order to better verify the effectiveness of the algorithm, ATO HILS is adopted in this paper to carry out simulation tests on the traditional improved evolutionary algorithm (MOEA/D), traditional improved shark smell optimization algorithm (CSSO) and the improved algorithm (ISSO) proposed in this paper. The ATO HILS results are shown in Fig. 11 to Fig. 14 and Table 4 to Table 6.

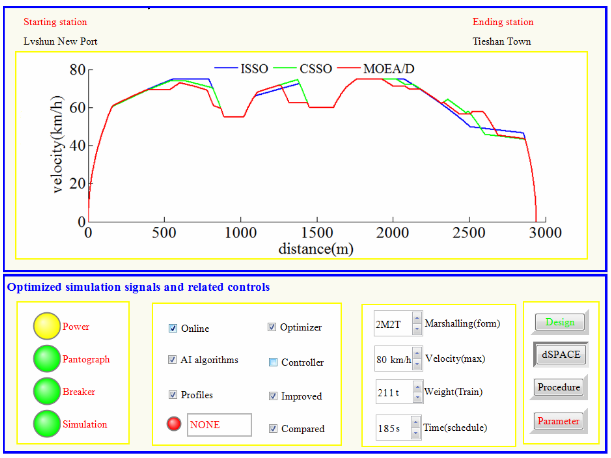

Fig. 11. The velocity distance profile of optimal results

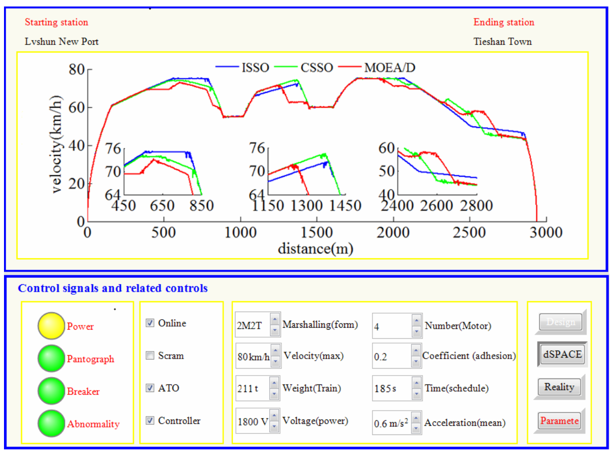

Fig. 12. The velocity distance trajectory of tracking control results

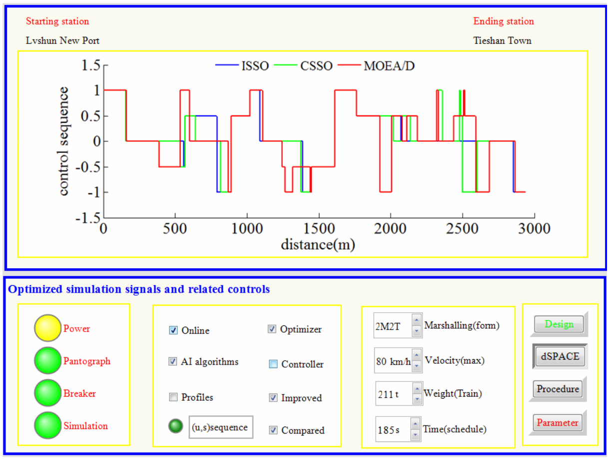

Fig. 13. The operating condition distance graph of optimal results

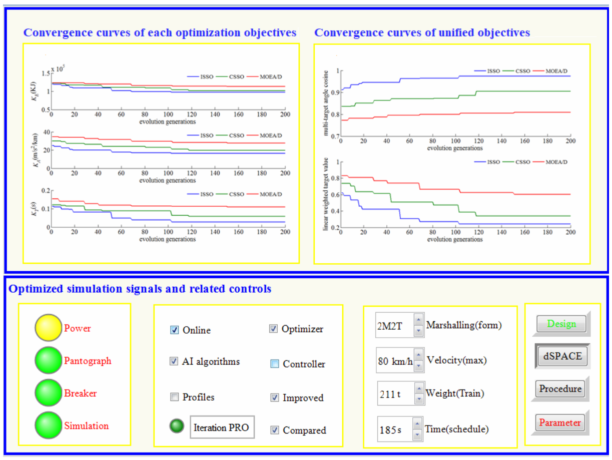

Fig. 14. Relevant evolution convergence curves of different algorithms

Table 4. Optimization results of different algorithms

Algorithm	Energy cosumption	Actual time	Comfort level	parking error
ISSO	97931KJ	185.0268s	5.5947m/s^2/km	0.0896m
CSSO	101793KJ	185.0585s	6.6586m/s^2/km	0.0941m
MOEA/D	113159KJ	185.1094s	9.4122m/s^2/km	0.1128m

Table 5. Evaluate results of different algorithms

Algorithm	Angle cosine	Linear weighted target
ISSO	0.9739	0.2428
CSSO	0.9051	0.3398
MOEA/D	0.8087	0.6014

Table 6. Tracking control results of different algorithms

Algorithm	Energy cosumption	Actual time	Comfort level	parking error
ISSO	106039KJ	185.0401s	37.6183m/s2/km	0.1319m
CSSO	118263KJ	185.0719s	46.3982m/s2/km	0.2109m
MOEA/D	131257KJ	185.1864s	55.6547m/s2/km	0.2895m

In Fig. 11 tp Fig. 14, the power is switched on, the pantograph is raised, and the circuit breaker is normally closed, which is in a normal simulation state. In Fig. 11, Fig. 13, Fig. 14 (which is related to the optimization of train operation process), the dSPACE simulator is in the working state (the ‘dSPACE’ button is pressed and the ‘Procedure’ button is waiting to be pressed), the human-computer interaction signal is normal (the ‘Design’ button is green), and the given parameters cannot be changed (the ‘Parameters’ button is red). In Fig. 12, the dSPACE simulator is in the simulation state (the ‘dSPACE’ button is pressed and the ‘Reality’ button is waiting to be pressed). In the tracking control state, the design parameters cannot be changed (the ‘Design’ button is white) and the given parameters cannot be changed (the ‘Parameters’ button is red).

According to simulation results of different algorithms from Table 2 to Table 6, compared with the traditional improved evolutionary algorithm (MOEA/D) and traditional improved shark smell optimization algorithm (CSSO), the improved algorithm proposed in this paper (ISSO) has the obvious performance improvement effect. The compared results with MOEA/D and CSSO of different simulation technologies are shown in Table 7.

Table 7. Compared with MOEA/D and CSSO of different simulation technologies

Algorithm	Energy cosumption	Actual time	Comfort level	parking error
Matlab	MOEA/D	7.70%	42.09%	42.52%
Matlab	CSSO	9.75%	24.58%	23.92%
HLS Optimized loop	MOEA/D	11.42%	75.68%	38.58%
HLS Optimized loop	CSSO	3.47%	34.79%	16.10%
HLS Control loop	MOEA/D	19.78%	76.78%	32.81%
HLS Control loop	CSSO	10.19%	36.68%	22.09%

As can be seen from the above ATO HILS results, the optimized profile and tracking control effect of improve by ISSO is ideal. This further demonstrates the effectiveness of the improvement strategy proposed in this paper.

6 Conclusion

Train multi-objective operation optimization is a very complex issue that needs to take into account the energy consumption, running time, comfort and so on and the ideal optimization solution is not easy to be obtained. An improved shark smell optimization algorithm based on angle cosine and fusion distance is proposed in this paper and the specific advantages are described below.

Compared to the traditional intelligent optimization algorithm, because of the unique spiral feeding mechanism of sharks, the shark smell optimization algorithm has stronger optimal searching ability, which is helpful to find more optimized solution.

For the multi-objective optimization problem, the evaluation index of the solution is very important. However, the linear weighted target belongs to the common multi-objective unified target, there is the problem that subjective parameters are selected blindly. In this paper, the multi-objective angle cosine is used as evaluation index, which can effectively avoid the blind selection of subjective parameters.

Because the updating rules of velocities and positions in the shark optimization algorithm make all individuals close to the extreme individuals, after a long iteration, the extreme individuals will form a certain degree of dominance over the population, which makes it difficult to converge globally. Therefore, in order to suppress the local convergence of shark optimization algorithm, it is necessary to determine accurately whether the individual aggregation occurs in shark populations. In this paper, the fusion distance can be used to take into account the relativity and independence of speed and time, which can detect whether there is the phenomenon of individual aggregation preciously, so the local convergence is better suppressed. Verified by the MATLAB simulation and ATO HILS, compared with the common optimization algorithm and conventional improved optimization algorithm, the improvement strategy proposed in this paper improves the calculation precision and optimization ability of the algorithm to a certain extent, which can get more ideal optimization results.

Acknowledgements

This research was supported by National Natural Science Foundation of China (60574018).

References

[1] K. Sindhya, K. Miettinen K,K. Deb, A hybrid framework for evolutionary multi-objective optimization, IEEE Transactions on Evolutionary Computation 17(4)(2013) 495-511.

[2] S. Wei, Y. Xi-Hui, C. Bai-Gen, W. Jang, Multiobjective optimization for train speed trajectory in ctcs high-speed railway with hybrid evolutionary algorithm, IEEE Transactions on Intelligent Transportation Systems 16(4)(2015) 2215-2225.

[3] C.S. Chang, D.Y. Xu, H.B. Quek, Pareto-optimal set based multi-objective tuning of fuzzy automatic train operation for mass transit system, IEE Proceedings-Electric Power Applications 146(5)(1999) 577-583.

[4] G. Qing, T. Tao, F. Ma, Energy-efficient train tracking operation based on multiple optimization models, IEEE Transactions on Intelligent Transportation Systems 17(3)(2015) 882-892.

[5] M. DomíNguez, A. FernáNdez-Cardador, A. Cucala, R. Pecharromán, Energy savings in metropolitan railway substations through regenerative energy recovery and optimal design of ATO speed profiles, IEEE Transactions on Automation Science and Engineering 9(3)(2012) 496-504.

[6] S. Yongduan, W. Song, A novel dual speed-curve optimization based approach for energy-saving operation of high-speed trains, IEEE Transactions on Intelligent Transportation Systems 17(6)(2016) 1564-1575.

[7] B. Yun, T.K. Ho, M. Baohua, C. Shaokuan, Energy-efficient locomotive operation for chinese mainline railways by fuzzy predictive control, IEEE Transactions on Intelligent Transportation Systems 15(3)(2014) 938-948.

[8] W. Pengliang, R.M.P. Goverde, Multiple-phase train trajectory optimization with signalling and operational constraints, Transportation Research Part C Emerging Technologies 69(2016) 255-275.

[9] V.A. Shim, K.C. Tan, H. Tang, Adaptive memetic computing for evolutionary multiobjective optimization, IEEE Transactions on Cybernetics 45(4)(2015) 610-621.

[10] T. González-Arteaga, J. Alcantud, R. Calle, A cardinal dissensus measure based on the Mahalanobis distance, European Journal of Operational Research, 251(2)(2016) 575-585.

[11] Z. Yuxiang, B. Du, Z. Liangpeng, W. Shugen, A low-rank and sparse matrix decomposition-based mahalanobis distance method for hyperspectral anomaly detection, IEEE Transactions on Geoscience & Remote Sensing 54(3)(2016) 1376-1389.

[12] G. Taguchi, Introduction to Quality Engineering: Designing Quality into Products and Processes, Asian Productivity Organization, Tokyo, 1986.

[13] L. Gang, W. Xingcheng, Fault diagnosis of diesel engine based on fusion distance calculation, in: Proc. Advanced Information Management, Communicates, Electronic and Automation Control Conference IEEE 2017, 2017.

[14] Z. Qingfu, L. Hui, MOEA/D: a multiobjective evolutionary algorithm based on decomposition, IEEE Transactions on Evolutionary Computation 11(6)(2008) 712-731.

[15] O. Abedinia, N. Amjady, Short-term wind power prediction based on hybrid neural network and chaotic shark smell optimization, International Journal of Precision Engineering and Manufacturing-Green Technology 2(3)(2015) 245-254.